
# A Burkholderia cenocepacia gene encoding a non-functional tyrosine phosphatase is required for the delayed maturation of the bacteria-containing vacuoles in macrophages

Andrade, A., & Valvano, M. A. (2014). A Burkholderia cenocepacia gene encoding a non-functional tyrosine phosphatase is required for the delayed maturation of the bacteria-containing vacuoles in macrophages. *Microbiology*. https://doi.org/10.1099/mic.0.077206-0

**Published in:**
Microbiology

**Document Version:**
Peer reviewed version

**Queen's University Belfast - Research Portal:**
Link to publication record in Queen's University Belfast Research Portal

**Publisher rights**
This is the author accepted manuscript version of this article that includes modifications to the paper based on referees' suggestions, but is prior to copy editing, typesetting and proof correction. The publisher version can be found at:
http://mic.sgmjournals.org/content/160/Pt_7/1332

**General rights**
Copyright for the publications made accessible via the Queen's University Belfast Research Portal is retained by the author(s) and / or other copyright owners and it is a condition of accessing these publications that users recognise and abide by the legal requirements associated with these rights.

**Take down policy**
The Research Portal is Queen's institutional repository that provides access to Queen's research output. Every effort has been made to ensure that content in the Research Portal does not infringe any person's rights, or applicable UK laws. If you discover content in the Research Portal that you believe breaches copyright or violates any law, please contact openaccess@qub.ac.uk.

Download date:05. May. 2023

# A *Burkholderia cenocepacia* gene encoding a non-functional tyrosine phosphatase is required for the delayed maturation of the bacteria-containing vacuoles in macrophages

**Angel Andrade[1] and Miguel A. Valvano[1,2*]**

[1] Centre for Human Immunology and Department of Microbiology and Immunology, University of Western Ontario, London, Ontario, Canada, N6A 5C1
[2] Centre for Infection and Immunity, Queen's University Belfast, Belfast, United Kingdom, BT9 5AE

* For correspondence: email, m.valvano@qub.ac.uk

Running Title: *Burkholderia* secreted protein affects endocytic traffic

Contents category: Microbial Pathogenicity
Number of words in the summary: 206
Number of words in the main text: 6164
Number of tables: 2
Number of figures: 9

**Abstract**

*Burkholderia cenocepacia* infects patients with cystic fibrosis. We have previously shown that *B. cenocepacia* can survive in macrophages within membrane vacuoles (BcCVs) that preclude fusion with the lysosome. The bacterial factors involved in *B. cenocepacia* intracellular survival are not fully elucidated. We report here that deletion of BCAM0628, encoding a predicted low-molecular weight protein tyrosine phosphatase (LMW-PTP) that is restricted to *B. cenocepacia* strains of the transmissible ET-12 clone, accelerates the maturation of the BcCVs. Compared to parental strain and deletion mutants in other LMW-PTPs that are widely conserved in *Burkholderia* species, a greater proportion of BcCVs containing the Δ*BCAM0628* mutant were targeted to the lysosome. Accelerated BcCV maturation was not due to reduced intracellular viability since Δ*BCAM0628* survived and replicated in macrophages similarly to the parental strain. Therefore, BCAM0628 was referred to as *dpm* (delayed phagosome maturation). We provide evidence that the Dpm protein is secreted during growth *in vitro* and upon macrophage infection. Dpm secretion requires an N-terminal signal peptide. Heterologous expression of Dpm in *B. multivorans* confers to this bacterium a similar phagosomal maturation delay as found with *B. cenocepacia*. We demonstrate that Dpm is an inactive phosphatase, suggesting that its contribution to phagosomal maturation arrest must be unrelated to tyrosine phosphatase activity.

## INTRODUCTION

The *Burkholderia cepacia complex* (Bcc) is a diverse group of at least 17 species widely distributed in the environment (Lipuma, 2005). Bcc species display extraordinary metabolic versatility and have the ability to colonize and adapt to various ecological niches (Coenye & Vandamme, 2003). Bcc strains are potentially beneficial bacteria to promote plant growth, pest control, and bioremediation (Parke & Gurian-Sherman, 2001). Unfortunately, Bcc are also opportunistic pathogens causing chronic infection in immunocompromised individuals such as those with chronic granulomatous disease and cystic fibrosis (Loutet & Valvano, 2010; Mahenthiralingam *et al.*, 2001; Vandamme *et al.*, 1997). *Burkholderia cenocepacia* and *Burkholderia multivorans* are the two Bcc species most commonly isolated worldwide from cystic fibrosis patients (Drevinek & Mahenthiralingam, 2010; Govan *et al.*, 2007).

Chronic infection with *B. cenocepacia* can result in acute, fatal necrotizing pneumonia and septicemia, termed "cepacia syndrome" (Courtney *et al.*, 2004; Mahenthiralingam *et al.*, 2008). Due to their intrinsic resistance to most available antibiotics the treatment of *Burkholderia* infections becomes difficult (George *et al.*, 2009; Waters & Ratjen, 2006). Macrophages are crucial in the early stage of host defense against infections; they ingest and destroy incoming pathogens upon phagocytosis and recruit inflammatory cells to the site of infection (Hume *et al.*, 2002; Kinchen & Ravichandran, 2008). Previous work has demonstrated that *B. cenocepacia* survive within a membrane-bound vacuole (hereafter referred as BcCV) in amoebae, human respiratory epithelial cells (Marolda *et al.*, 1999; Saldias & Valvano, 2009) and macrophages (Hamad *et al.*, 2010; Lamothe *et al.*, 2007). Intramacrophage survival of *B. cenocepacia* has been associated with an arrest of the phagosomal maturation, since the BcCV shows impaired acidification and delayed fusion with lysosomes during the initial 6-8 h post infection (Huynh *et al.*, 2010; Lamothe *et al.*, 2007; Lamothe & Valvano, 2008). The delayed fusion of the BcCV with lysosomes can be attributed, at least in part, to impaired assembly of the NADPH oxidase complex on the BcCV membrane (Keith *et al.*, 2009) as consequence of Rac1 inactivation (Flannagan *et al.*, 2012; Rosales-Reyes *et al.*, 2012b). Inactivation of Rab7 (Huynh *et al.*, 2010), a small GTPase important for the endosome maturation (Wang *et al.*, 2011), is also critical for this delay. Furthermore, recent evidence indicates that the BcCV can lose membrane integrity resulting in bacteria coming into contact with cytosol components (Al-Khodor *et al.*, 2013) and promoting macrophage cell death by pyroptosis (Rosales-Reyes *et al.*, 2012a). Loss of BcCV permeability partly depends on the activity of a type VI secretory system, while effector proteins secreted by a Type II secretory pathway can alter the BcCV maturation (Rosales-Reyes *et al.*, 2012a). These observations suggest a complex interplay of *B. cenocepacia* effectors contributed by at least two different secretory pathways in the manipulation of the vesicular trafficking in macrophages. However, the specific bacterial components required are largely unknown.

Protein tyrosine phosphorylation is a covalent modification that regulates numerous cellular functions in eukaryotic and bacterial cells (Cozzone *et al.*, 2004). Bacterial tyrosine kinases catalyze the phosphorylation of the side hydroxyl groups of tyrosine residues in protein substrates leading to the formation of the corresponding phosphomonoesters (Shi *et al.*, 1998), while bacterial protein tyrosine phosphatases (PTPs) catalyze the reverse reaction. Bacterial PTPs can be categorized based on structural basis into three subfamilies: (i) the low molecular weight protein-tyrosine phosphatases (LMW-PTPs), composed by small and acidic enzymes

present also in eukaryotes; (ii) the classic type I Cys-based PTPs, also known as eukaryotic-like phosphatases (Böhmer *et al.*, 2013); and (iii) the polymerase and histidinol phosphatase family of phosphoesterases, which is found mainly in Gram-positive bacteria (Morona *et al.*, 2002). Bacterial PTPs operate in two major processes: production and translocation of exopolysaccharides (reviewed in (Cozzone *et al.*, 2004)), and interference with host signal transduction upon infection (Cozzone, 2005; Whitmore & Lamont, 2012). Examples of PTPs affecting host signaling pathways include YopH from *Yersinia*, which is injected into human epithelial cells where it targets host focal adhesion proteins, such as p130Cas, paxillin, and focal adhesion kinase (FAK) (Black & Bliska, 1997; Persson *et al.*, 1997). Similarly, SptP from *Salmonella enterica* serovar Typhimurium inhibits the activation of the MAPK pathway by dephosphorylating Raf (Lin *et al.*, 2003), disrupts the intermediate filaments distribution after vimentin binding (Murli *et al.*, 2001), and regulates the biogenesis of an intracellular niche through VCP dephosphorylation (Humphreys *et al.*, 2009). *Mycobacterium tuberculosis* secretes two PTPs, both required for intracellular survival in macrophages. PtpA inhibits V-ATPase trafficking to the mycobacterial phagosome and blocks phagolysosome fusion (Bach *et al.*, 2008; Wong *et al.*, 2011), while PtpB has a possible role subverting the host immune response (Zhou *et al.*, 2010).

Manipulation of host signal transduction pathways by intracellular *B. cenocepacia* strongly suggests that bacterial secreted virulence factors are operating to allow the subversion of the host cell (Abdulrahman *et al.*, 2013; Rosales-Reyes *et al.*, 2012a). On this basis, we evaluated four predicted LMW-PTPs: BCAM0208, BCAM0628, BceD and BCAL2200, for their contribution to intracellular survival and phagosome maturation arrest. We demonstrate that *B. cenocepacia* secretes BCAM0628 (herein designated as *dpm* (delayed phagosome maturation) during growth and upon macrophage infection. Deletion of *dpm* accelerates the maturation of the BcCVs. Translocation of Dpm requires an N-terminal signal peptide plus an unperturbed C-terminal region. We also demonstrate that Dpm is an inactive phosphatase, suggesting that the maturation arrest of phagocytic vacuoles is unrelated to tyrosine phosphatase activity.

## METHODS

**Bacterial strains, plasmids and growth conditions.** Bacterial strains and plasmids used here are listed in Table 1. Bacteria were cultured in Luria broth (LB; Difco) at 37 °C with shaking. *Escherichia coli* cultures were supplemented, as required, with the following antibiotics (final concentrations): tetracycline (25 μg $ml^{-1}$), kanamycin (40 μg $ml^{-1}$), trimethoprim (50 μg $ml^{-1}$) and chloramphenicol (30 μg $ml^{-1}$). *B. cenocepacia* cultures were supplemented, as required, with trimethoprim (100 μg $ml^{-1}$), tetracycline (100 μg $ml^{-1}$), and chloramphenicol (120 μg $ml^{-1}$). To assess growth rates of parental and mutant strains of *B. cenocepacia* MH1K, overnight cultures were inoculated into fresh medium to give a starting optical density at 600 nm ($OD_{600}$) of 0.01. Growth rates were determined in 100-well microtiter plates using a Bioscreen C automated microbiology growth curve analysis system (MTX Lab Systems, Inc.). *E. coli* strains for cloning and production of recombinant proteins were DH5α and BL21(DE3), respectively. *E. coli* GT115 was used for cloning into the suicide vector pGPI-SceI.

**General molecular techniques.** DNA manipulations and cloning were performed as described previously (Sambrook & Russell, 2001). PCR amplification was performed using *Taq* or HotStar HiFidelity DNA polymerases (Qiagen). Antarctic phosphatase (New England Biolabs), restriction enzymes (New England Biolabs) and T4 DNA ligase (Roche Applied Science) were used as recommended by the manufacturers. DNA sequencing was completed at the sequencing facility in York University (Toronto, Canada) and in Eurofins MWG Operon (Alabama, USA). Plasmids were mobilized into *B. cenocepacia* and *B. multivorans* by triparental mating (Craig *et al.*, 1989; Figurski & Helinski, 1979).

**Mutagenesis of *B. cenocepacia* K56-2.** The construction of unmarked, non-polar mutant strains was accomplished as described (Flannagan *et al.*, 2008). The deletion mutagenesis plasmids were created by amplifying 400-550 bp DNA fragments flanking the corresponding target genes using chromosomal DNA from *B. cenocepacia* K56-2 as template and the indicated primer pairs (Table 2). The amplicons were double digested with the corresponding restriction enzymes (Table 2) and cloned into pGPISce-I resulting in mutagenic plasmids pDelM0208, pDelM0628, pDelM0857 and pDelL2200 (Table 1). Mutagenic plasmids were mobilized into *B. cenocepacia* MH1K strain by triparental mating and co-integrants were selected using 100 μg $ml^{-1}$ trimethoprim. Selection against the *E. coli* donor and helper strains after the triparental mating was accomplished using 100 μg $ml^{-1}$ ampicillin in combination with 25 μg $ml^{-1}$ polymyxin B. pDAI-Sce-I-SacB, used in the final stage of mutagenesis to induce the second recombination event leading to an unmarked gene deletion, was mobilized into *B. cenocepacia* co-integrants. Exconjugants were selected with 100 μg $ml^{-1}$ tetracycline, 100 μg $ml^{-1}$ ampicillin, and 25 μg $ml^{-1}$ polymyxin B. Identification of the appropriate gene deletions was accomplished by PCR. Deletion mutants were cured of the levansucrase (SacB)-encoding plasmid by growing the *B. cenocepacia* mutant strains in LB broth overnight and then plating on LB agar supplemented with 5% (w/v) sucrose.

**Motility assays.** For swimming assays, 2 μl of overnight culture, adjusted to an $OD_{600}$ of 1.0, was inoculated within the agar of a swim plate (LB; 0.3% agar). For swarming assays, 2 μl of overnight culture, adjusted to an $OD_{600}$ of 1.0, was spotted on top of the swarm plate agar (nutrient broth; 0.5% agar, 0.2% glucose). The plates were incubated at 37 °C for 24 h, after which the diameters of the swimming and swarming zones were measured.

**Cloning of predicted phosphotyrosine phosphatase genes and site-directed mutagenesis.** The open reading frames BCAM0208, *bceD*, BCAL2200 and the full length *dpm* or the *dpm* truncated version were PCR-amplified using chromosomal DNA from *B. cenocepacia* K56-2 as template with the corresponding primer pairs (Table 2). Amplicons were digested with the restriction enzymes *Nde*I-*Xba*I and cloned into a similarly digested pDA17 plasmid, giving rise to pM0208, pbceD, pL2200, pdpm and pΔ27 (Table 1). To produce histidine tagged recombinant proteins, Dpm and BCAL2200 the plasmids pdpm or pL2200 were digested with *Nde*I-*Hind*III and the resulting inserts were cloned into a similarly digested pET28a plasmid, giving rise to pHisdpm and pHisL2200, respectively. To generate pdpmHis, *dpm* was amplified from chromosomal DNA with the primer pair 6829-6830 (Table 2), the PCR product was digested with *Nco*I-*Xho*I and cloned into a similarly digested pET28a. The site directed mutagenesis of *dpm* was performed by PCR with *Pfu* DNA polymerase (Stratagene) using the primer pair 6496-6517 (Table 2) and the plasmid pHisdpm or pdpmHis as template for the reaction. *Dpn*I was

added to PCR reactions for overnight digestion of parental plasmid DNA at 37 °C. The resulting DNA was introduced into *E. coli* DH5α by transformation, and transformants were selected on LB-agar containing 40 μg $ml^{-1}$ kanamycin. Directed mutagenesis in the resulting plasmids, pHisdpm D36C and pdpmHis D36C (Table 1), respectively, was confirmed by sequencing.

**Protein analysis.** Overnight cultures were diluted 1:100 in 7 ml of LB. After 2 h of incubation at 37 °C, the cultures were centrifuged for 15 min at 16,100 ×*g* and the resulting pellets were resuspended in 1× SDS–PAGE sample buffer; the volume was normalized to the $OD_{600}$. Supernatants were sterilized through a 0.22-μm filter (Millipore), and proteins were precipitated during 4 h at 4 °C with 10% (vol/vol) of trichloroacetic acid (final concentration). The precipitates were isolated by centrifugation at 16,100 ×*g* for 30 min at 4 °C, and the pellet was air-dried and resuspended in 2× SDS–PAGE sample buffer containing 10% (vol/vol) of saturated Tris base. Protein concentration of the different cultures was normalized to the $OD_{600}$ value. After SDS–PAGE, the gel was transferred onto a nitrocellulose membrane. The membrane was then blocked overnight with western blocking reagent (Roche Diagnostics) in TBST (50 mM Tris-HCl pH 7.5, 150 mM NaCl, 0.1 % Tween-20). The primary antibodies, anti-FLAG M2 monoclonal antibody (Sigma) or anti-αRNAPol (*E. coli*) (Neoclone), were diluted to 1:15,000 in TBST, anti-beta lactamase (TEM-1, *E. coli*) (Thermo Fisher) was diluted to 1:5,000 in TBST. Primary antibodies were applied for 1.5 h. Secondary antibody, goat anti-mouse Alexa Fluor 680 IgG antibodies (Invitrogen), was diluted to 1:15,000 and applied for 1 h. Western blots were developed using LI-COR Odyssey infrared imaging system (LI-COR Biosciences, Lincoln, NE).

**Intracellular survival in macrophages.** Bacterial intracellular survival in RAW264.7 murine macrophages was assayed as described previously (Schmerk & Valvano, 2013). Bacteria were added to macrophages at multiplicity of infection (MOI) of 50. Plates were centrifuged for 1 min at 300 × g and incubated for 2 h at 37 °C under 5% $CO_2$. Infected macrophages were washed with PBS three times to remove extracellular bacteria and fresh medium containing 100 μg $ml^{-1}$ gentamicin was added to kill any remaining extracellular bacteria. After 1 h, the macrophages were washed twice in PBS, and fresh medium containing 10 μg $ml^{-1}$ gentamicin was added for the remainder of the experiment. To enumerate intracellular bacteria infected macrophages were lysed with 0.1% sodium deoxycholate (w/v), and the lysates were serially diluted in PBS before plating on LB agar.

**Phagosomal maturation assays.** For lysosome labeling, macrophages were incubated overnight with 250 μg $ml^{-1}$ fluorescein isothiocyanate–dextran (Invitrogen). External fluorescein–dextran was removed by serial washes with PBS and chased for 1 h in fresh medium. Infections of RAW264.7 macrophages with B. cenocepacia strains carrying pIN62 (for bacteria labeling) or B. multivorans ATCC 17616 Gms carrying pDA17 or pdpm were performed as described above. After infection extracellular bacteria were removed by washes and fresh medium containing 50 μg $ml^{-1}$ gentamicin was added. At 2 h post infection cells were fixed at room temperature for 25 min using 4% (v/v) paraformaldehyde and visualized at × 100 magnification. The *B. multivorans* infected macrophages were similarly treated but the infection proceeded during 1 h, similarly to (Schmerk & Valvano, 2013). For immunostaining, fixed cells were permeabilized using 0.1% (v/v) Triton X-100 at room temperature for 30 min. Coverslips were blocked in a solution of 3% (w/v) BSA, 2% (v/v) FBS in PBS for 2 h at 4 °C. The coverslips were then incubated at 4 °C overnight with rat anti-lysosome-associated membrane protein-1 (LAMP-1) (clone 1D4B; BD

Pharmingen) at a 1:200 dilution, for complementation assays due to plasmid incompatibly bacteria were labeled with rabbit antiserum against *B. cenocepacia* K56-2 (Rosales-Reyes *et al.*, 2012b) at a 1:4 000 dilution. Alexa Fluor 488-labelled chicken anti-rat (Invitrogen) and Alexa Fluor 594-labelled goat anti-rabbit (Invitrogen), when necessary, were added at a 1:4 000 dilution for 90 min prior to visualization at × 100 magnification. Fluorescence and phase-contrast images were acquired using a QImaging RETIGA-SRV camera on an Axioscope 2 (Carl Zeiss) microscope.

**Intramacrophage Dpm secretion.** RAW264.7 macrophages were infected with *B. cenocepacia* Δ*dpm* strain carrying the plasmid pdpm or pΔ27 (Table 1) as described above. At 1 h post infection cells were fixed and treated as described for immunostaining. The coverslips were then incubated at 4 °C overnight with mouse anti-FLAG M2 monoclonal antibody (Sigma) at a 1:200 dilution and with rabbit antiserum against *B. cenocepacia* K56-2 at a 1:4 000 dilution. Then Alexa Fluor 488-labelled goat anti-mouse (Invitrogen) and Alexa Fluor 594-labelled goat anti-rabbit (Invitrogen) were added at a 1:4 000 dilution for 90 min prior to visualization at × 100 magnification.

**Production and purification of recombinant proteins.** Plasmids pHisdpm, pHisL2200 and pdpmHis (Table 1) were expressed in *E. coli* BL21(DE3). 200 ml LB cultures were growth at 30°C until they reached an $OD_{600}$ 0.7. Then 0.3 mM IPTG (isopropyl-β-D-thiogalactopyranoside) was added and bacteria continued growing for 4 h. Induced bacteria were harvested by centrifugation and bacterial pellets were resuspended in binding buffer, BB (20 mM Tris–HCl, pH 8.0, 0.5 M NaCl) containing protease inhibitor cocktail (Roche Diagnostics). Cell lysis was achieved using a cell disruptor (Constant Systems Ltd) at 20 kpsi. Lysates were centrifuged for 50 min at 24,000 ×g, 4 °C, to pellet undisrupted cells and inclusion bodies. Soluble fractions were applied to $Ni^{2+}$ charged sepharose beads for 30 min at 4 °C. After extensive washing with BB containing 40 mM imidazole, proteins were eluted with BB containing 200 mM imidazole. Purified recombinant proteins were dialyzed overnight at 4 °C against 1.0 l of TND buffer (50 mM Tris–HCl, pH 8.0, 100 mM NaCl and 1 mM DTT). Protein concentration was determined by using the Bio-Rad protein assay dye-binding reagent (Bio-Rad).

**Phosphatase activity.** Phosphatase activity was determined by monitoring, at 405 nm, the *p*-nitrophenol (PNP) formed from *p*-nitrophenol phosphate (PNPP) as previously described in (Cowley *et al.*, 2002) with minor modifications. Mixtures reaction contained, in a final volume of 1 ml, 2.5 µg of purified and dialyzed protein in 7 mM HEPES pH 7.0, 5 mM $MgCl_2$ and 1 mM DTT. Enzymatic reactions were started adding 1 mM PNPP and incubated at 37 °C. After the determinate time intervals reactions were stopped adding 0.2 N NaOH (final concentration) and the absorbance was measured at 405 nm. The concentration of PNP formed was estimated using a molar extinction coefficient of $1.78 \times 10^4$ $M^{-1}$ $cm^{-1}$. And phosphatase activity was calculated from the slope obtained in time course analyses.

**Statistical analyses.** All experiments were performed at least in triplicate. All data are presented as means ± SEM of the indicated number of experiments. Statistical analyses were done by Student's t-test and one-way analysis of variance for comparisons of means using GraphPad Prism version 4.03.

## RESULTS

### Identification of *B. cenocepacia* putative LMW-PTPs

Analysis of the *B. cenocepacia* J2315 genome (J2315 is clonally related to strain K56-2) with Conserved Domain Database (Marchler-Bauer *et al.*, 2011) tools revealed 4 open reading frames encoding proteins with putative LMWPc domains (pfam01451). These enzymes catalyze the removal of a phosphate group attached to a tyrosine residue, using a cysteinyl-phosphate enzyme intermediate (Wang *et al.*, 2000). The predicted LMW-PTPs were BCAL2200, BCAM0208, BCAM0628 (Dpm) and BCAM0857 (BceD). The genes encoding these proteins are located in different clusters within the first (BCAL) and second (BCAM) chromosomes (Fig. 1). The cluster containing *bceD* was previously identified as part of the *bce* exopolysaccharide biosynthetic gene cluster (Moreira *et al.*, 2003), which is widespread within all the sequenced *Burkholderia* strains, with the exception of *B. rhizoxinica and B. mallei* (Ferreira *et al.*, 2010). BCAM0208 resides in another exopolysaccharide biosynthesis cluster next to the predicted tyrosine kinase BCAM0207 (Fig. 1b), in a similar arrangement as the described *bceD/bceF* pair of genes (Moreira *et al.*, 2003). BCAM0208/BCAM0207 are also widespread in the *Burkholderia* genus. BCAL2200 is located within a region highly conserved in other *Burkholderia* species, which presumably is involved in regulating sulfur amino acid metabolism (Fig. 1b and data not shown). In contrast, *dpm* is located in a poorly conserved region of the genome, and homologues to *dpm* are only found in *B. cenocepacia* J2315, K56-2, and H111, as well as in *B. cepacia* GG4 and *B. lata* (Fig. 1b and data not shown). Analysis of the translated sequences of *B. cenocepacia* LMW-PTPs showed a common secondary structure prediction pattern (data not shown) and indicated that all except Dpm have the conserved amino acids of the tyrosine phosphatase motif, $CX_5R(S/T)$ (Fig. 1a). Dpm has an aspartate substitution in the position of the catalytic cysteine (Fig. 1a) and a larger N-terminus with strong prediction to a signal peptide sequence (data not shown), suggesting it is a secreted protein.

### Dpm is secreted to the growth medium

The genes encoding BCAM0208, Dpm, BceD and BCAL2200 were cloned into pDA17 under the expression of the constitutive *dhfr* promoter. Resulting plasmids, pM0208, pdpm, pbceD and pL2200 (Table 1) were mobilized into *B. cenocepacia* K56-2 and secretion assays were performed as described in Methods. The pDA17 vector enables to fuse a C-terminal FLAG tag, which facilitates detection of the expressed products by immunoblotting. Our results show that except for BceD, the other proteins had similar expression levels (Fig. 2, upper left panel), as compared to the β-lactamase TEM-1, which was used as a loading control (Fig. 2, lower left panel). However, only Dpm was found in the supernatant (Fig. 2, upper panels). The absence of TEM-1 in supernatants (Fig. 2, lower panels) rules out spontaneous cell lysis or outer membrane leakage, confirming that Dpm is a secreted protein. Also, we did not find cytoplasmic RNA polymerase α-subunit in supernatants (data not shown), which provided an additional control indicating the cell lysis, did not occur during these experiments.

### Characterization of *B. cenocepacia* tyrosine phosphatase mutants

Single gene deletion mutants of BCAM0208, *dpm*, *bceD* and BCAL2200 were constructed to evaluate the contribution of individual LMW-PTPs to *B. cenocepacia* infectivity in

316 macrophages. The genetic background for the construction of the mutants was *B. cenocepacia*
317 MH1K, an aminoglycoside sensitive K56-2 mutant strain useful for intracellular infections
318 (Hamad *et al.*, 2010). No differences in growth rate at 37 or 42 °C were found in the
319 Δ*BCAM0208*, Δ*dpm*, Δ*bceD* and Δ*BCAL2200* mutants in comparison to parental MH1K (Fig.
320 3a). Also, the mutants did not differ in swimming and swarming motility (Fig. 3b), except for
321 Δ*bceD*, which had a noticeable swarming defect (Fig. 3b).
322
323 **Δ*dpm* cannot delay BcCV lysosomal fusion**
324 We have previously reported that the BcCV in infected macrophages has a maturation arrest
325 demonstrated by failure to acidify and delayed fusion with lysosomes up to 6-8 h post infection
326 (Huynh *et al.*, 2010; Lamothe *et al.*, 2007; Lamothe & Valvano, 2008). To determinate whether
327 vacuoles containing *B. cenocepacia* mutant strains display delayed phagosome maturation we
328 preloaded macrophages with fluorescein isothiocyanate–dextran overnight prior to infection with
329 parental and mutant bacteria. At 2 h post infection, BcCVs in Δ*dpm* infected macrophages
330 showed significant differences in colocalization with the fluorescein-labelled lysosomes (Fig.
331 4a). Quantification indicated that 66 ± 2 % of BcCVs containing Δ*dpm* were dextran positive,
332 while 40 ± 2 % of BcCVs containing the parental strain colocalized with dextran rich
333 compartments ($p<0.01$; Fig. 4b). In contrast, BcCVs of macrophages infected with Δ*BCAM0208,*
334 Δ*bceD* and Δ*BCAL2200* indicated 27 ± 6 %, 39 ± 4 % and 39 ± 2 % colocalization with dextran
335 (Fig. 4b). These results suggest that loss of Dpm increases the traffic of BcCVs to the lysosome.
336
337 To further characterize the differential endocytic trafficking observed in macrophages infected
338 with Δ*dpm* we compared the accumulation of the lysosome-associated membrane protein
339 (LAMP-1) on the BcCVs by immunostaining (Fig. 5a). At 2 and 4 h postinfection, 47 ± 3 and 59
340 ± 1.5% of BcCVs containing Δ*dpm* accumulated LAMP-1, respectively (Fig. 5b). In contrast, 30
341 ± 0.5 and 32 ± 7 % of BcCVs containing the parental strain colocalized with LAMP-1 (Fig. 5b),
342 respectively, as it has been previously shown for *B. cenocepacia* strains (Schmerk & Valvano,
343 2013). LAMP-1 accumulation of Δ*dpm* BcCVs was restored to parental levels (25 ± 3 % and 45
344 ± 3 % after 2 and 4 h, respectively) by expressing *dpm* from the pdpm plasmid (Fig. 5a and b).
345 Together, these results indicate that Dpm contributes to the delayed phagolysosomal fusion in
346 macrophages infected with *B. cenocepacia*.
347
348 **Dpm is secreted intracellularly upon macrophage infection**
349 We tested whether $Dpm_{FLAG}$ is secreted after bacterial internalization by macrophages using
350 antiserum against *B. cenocepacia* in combination with monoclonal antibodies against the FLAG
351 epitope. Macrophages were infected with Δ*dpm* carrying pdpm (encoding full length Dpm), or
352 pΔ27 (encoding Dpm lacking the predicted leader peptide Table 1). Immunostaining of
353 macrophages infected with Δ*dpm* (pdpm) revealed FLAG-specific immunofluorescence at the
354 periphery of 62.74 ± 2.2 % BcCVs, which overlapped with the localization of *B. cenocepacia*
355 (Fig. 6a and b), as expected by a secreted effector able to escape from the phagosome (Bach *et*
356 *al.*, 2008). In contrast, only 5.4 ± 0.2 % of FLAG-specific signal was observed colocalizing with
357 BcCVs of macrophages infected with Δ*dpm* (pΔ27) (Fig. 6a and b), this value can be attributed
358 to the detergent treatment during permeabilization for immunostaining or even to bacteria cell
359 lysis. Immunoblot analysis of bacterial lysates revealed that *dpm* and Δ27*dpm* were equally
360 expressed (Fig. 6c, left upper panel), confirming that both proteins are synthesized at similar
361 levels. We also noticed that $\Delta 27Dpm_{FLAG}$, which has a predicted mass of 18 kDa, migrated

slightly above full-length $Dpm_{FLAG}$, which has a predicted mass of 20.9 kDa (Fig. 6c, upper panel). We interpreted this result as an indication of the presence of uncleaved $\Delta 27Dpm_{FLAG}$ polypeptide and efficiently processed $Dpm_{FLAG}$. This is supported by the demonstration that $Dpm_{FLAG}$ but not the truncated derivative was detected in the culture supernatants (Fig. 6c, upper panel). The lack of β-lactamase TEM-1 in the supernatants indicated that the bacteria had an intact outer membrane leakage (Fig 6c, lower panel). Together, our results indicate that Dpm requires an N-terminal (signal peptide) for secretion.

**Single LMW-PTPs are not required to *B. cenocepacia* intramacrophage survival**

We also assessed whether the effect of Δ*dpm* in the acceleration of the BcCV maturation correlates with decreased intracellular bacterial survival. Gentamicin protection assays of macrophages infected with Δ*BCAM0208*, Δ*dpm*, Δ*bceD*, and Δ*BCAL2200* revealed no differences in the recovery of intracellular bacteria at 1 h and 24 h post infection in comparison to the parental strain (Fig. 7). Similar results were also obtained using human THP-1 macrophages (data not shown), a more restrictive cell line to *B. cenocepacia* infection (Schmerk & Valvano, 2013). Therefore, none of the LMW-PTPs encoding genes is required for *B. cenocepacia* intramacrophage survival.

**Dpm delays maturation of *B. multivorans*-containing vacuoles (BmCVs)**

Unlike *B. cenocepacia*, *B. multivorans* strains do not delay phagosomal maturation in murine macrophages (Schmerk & Valvano, 2013). No homolog to *dpm* is present in the *B. multivorans* ATCC 17616 genome (data not shown). To investigate whether Dpm could alter *B. multivorans* trafficking pdpm and pDA17 (vector control) were mobilized into *B. multivorans* ATCC 17616 $Gm^S$ (Table 1) and these strains were used in infection experiments. Macrophages were preloaded with fluorescein isothiocyanate–dextran and subsequently infected with ATCC 17616 $Gm^S$ (pDA17) or ATCC 17616 $Gm^S$ (pdpm). At 2 h post infection, 45 ± 0.2% of BmCVs carrying ATCC 17616 $Gm^S$ (pdpm) colocalized with fluorescent dextran. In contrast, colocalization with fluorescent dextran was observed in 74 ± 0.4% of ATCC 17616 $Gm^S$ (pDA17) BmCVs (Fig. 8a and b). Furthermore, we confirmed that *B. multivorans* supports the secretion of Dpm, as demonstrated by detection of this protein in the supernatant of *B. multivorans* at similar levels as found with *B. cenocepacia* (Fig. 8c). Together, the results of these experiments strongly support the notion that Dpm is a bacterially secreted protein affecting phagosomal maturation.

**Dpm lacks phosphatase activity**

Despite the absence of a critical Cys for catalysis in its predicted phosphatase motif we investigated if the Dpm has any phosphatase activity. We constructed inducible plasmids encoding N- or C-terminal histidine tagged Dpm (pHisdpm and pdpmHis, respectively, since the position of the histidine tag may alter phosphatase activity (Ueda & Wood, 2009). A plasmid expressing BCAL2200 carrying an N-terminal 6x-His tag (pHisL2200) was used as a control. Recombinant proteins were overproduced in *E. coli* BL21(DE3) and purified by $Ni^{2+}$-affinity chromatography (Fig. 9a). A double banded pattern appeared using Dpm-His (carrying a C-terminal His tag), suggesting the purification of both processed and unprocessed forms of Dpm, which agreed with the predicted masses of 20.9 and 17.9 kDa, respectively (Fig. 9a). In contrast, the presence of the histidine tag plus 10 additional residues in the Dpm N-terminus blocks processing of the protein resulting in a polypeptide with an apparent mass of 24 kDa, as expected

(Fig. 9a). All of the purified proteins were assayed for their ability to cleave the general phosphatase substrate *p*-nitrophenyl phosphate (PNPP). Recombinant BCAL2200 efficiently hydrolyzed the synthetic substrate (Fig. 9b) with an estimated specific activity of 1.44 ± 0.4 nmoles $min^{-1}$ $\mu g^{-1}$, a value that is in the range of that reported for other bacterial LMW-PTPs (Ferreira *et al.*, 2007; Vincent *et al.*, 1999). However, we could not detect PNPP hydrolysis by any of the Dpm derivatives under the same conditions used for BCAL2200 or by adding a 10-fold excess of substrate and/or protein into the reaction mix (Fig. 9b and data not shown). We attempted the reconstruction of the catalytic site by replacing the aspartate at position 36 with cysteine. The corresponding recombinant proteins His-$Dpm_{D36C}$ and Dpm-$His_{D36C}$ were purified to homogeneity (Fig. 9a) and assayed for PNPP hydrolysis, but they remained inactive (Fig. 9b). Together, these experiments indicate that Dpm lacks phosphatase activity, but this is not only due to the absence of a cysteine at the D36 position (Fig. 9b), suggesting additional mutations in this protein that alter its putative phosphatase activity.

## DISCUSSION

Persistence of *B. cenocepacia* and other Bcc bacteria within the airways of cystic fibrosis patients has been associated with their ability to survive intracellularly in macrophages and epithelial cells (Valvano *et al.*, 2014). We have previously shown abnormal maturation of the BcCVs in infected macrophages, but very little is known about the mechanism used by intracellular *B. cenocepacia* to arrest phagolysosome fusion. In this work, we show that deletion of *dpm* accelerates the maturation of the BcCVs in macrophages cells.

Dpm was initially identified as one member of a group of four predicted LMW-PTPs in *B. cenocepacia*. These putative proteins were investigated since bacterial protein tyrosine phosphatases commonly interfere with host signaling (Whitmore & Lamont, 2012) and could be candidates for effector proteins mediating the phagosomal maturation arrest in *B. cenocepacia*-infected macrophages. However, *dpm* was the only gene whose deletion resulted in loss of the phagosomal maturation defect in *B. cenocepacia*-infected macrophages. Several pieces of evidence support this conclusion: (i) the Δ*dpm* strain rapidly acquired the lysosomal marker LAMP-1, a phenotype that was abrogated by restoration of a functional *dpm* expressed from a recombinant plasmid; (ii) BcCVs containing Δ*dpm* bacteria colocalized more rapidly with dextran rich compartments; and (iii) heterologous expression of *dpm* in *B. multivorans*, which normally traffics rapidly to the lysosome, caused a delay in the traffic of bacteria-containing vacuoles to the lysosome compartment. Together, these observations indicate that Dpm directly contributes to the phagosome maturation arrest observed for intracellular *B. cenocepacia*.

The role of Dpm as an effector protein is also supported by its ability to be secreted to the culture supernatant and in macrophages. Indeed, Dpm was the only predicted tyrosine phosphatase that was secreted both *in vitro* and also during macrophage infection, as it could be detected at the periphery of the BcCVs. Deletion experiments revealed that Dpm secretion requires a signal peptide, suggesting that the protein crosses the inner membrane in a Sec-dependent manner. The specific mechanism involved in Dpm secretion across the outer membrane remains to be discovered. Nevertheless, once Dpm is transported outside the bacteria we can hypothesize that it escapes of the vacuole through the BcCV membrane damage induced via T6SS, in a similar

manner as has been shown for type II secreted proteins (Rosales-Reyes *et al.*, 2012a). Despite the relevance of Dpm delaying phagosome maturation, bacterial intramacrophage survival was not affected in the Δ*dpm* strain suggesting that other factors are required to enable *B. cenocepacia* survival in the lysosomes. The trafficking delay in *B. cenocepacia* is not observed with *B. multivorans* although both bacteria can survive in a lysosomal compartment (Schmerk & Valvano, 2013). This suggests that other factors likely common to both species play a role in intramacrophage survival. A similar scenario can be anticipated to other Bcc members; however additional work describing specific intracellular behavior of different Bcc members remains to be revealed.

The apparently restricted conservation of *dpm* to only a few *Burkholderia* species is puzzling. This gene in *B. cenocepacia* is located next to BCAM0627, encoding a putative endonuclease VII protein that is homologous to gp-49 from the T4 phage, which resolves four-way junctions in branch DNAs (Jensch & Kemper, 1986). BCAM0627 is predicted to be co-transcribed with BCAM0626, which encoded a helix-turn-helix protein. Both BCAM0626-BCAM0627 form a predicted toxin-antitoxin cassette, which is proposed to stabilize heterologous replicons (Dziewit *et al.*, 2007). Therefore, it is possible that *dpm* and its neighboring genes may have been acquired by horizontal transmission, thus explaining their restricted conservation.

Remarkably, Dpm lacks phosphatase activity and this defect cannot be corrected by reconstructing the critical catalytic cysteine at the position corresponding to aspartate 36. However, a highly conserved second cysteine and a proline at positions 41 and 44, respectively, are also missing in the Dpm predicted phosphatase motif. These residues could also be important for proper enzymatic activity, since both cysteines of the phosphatase motif may form an intramolecular disulfide bridge that protects the nucleophilic cysteine from oxidation (Raugei *et al.*, 2002). Alternatively, other mutations abolishing phosphatase activity appear to stabilize substrate binding (Bach *et al.*, 2008; Bliska *et al.*, 1992; Mukhopadhyay & Kennelly, 2011; Murli *et al.*, 2001). Therefore, we speculate that Dpm could potentially recognize and remain attached to a tyrosine phosphorylated host cell substrate, partially blocking its function. Another possibility is that Dpm might recognize a non-tyrosine phosphorylated host substrate. For instance PtpA from *M. tuberculosis* prevents phagosomal acidification by binding to the H-subunit of the macrophage vacuolar-$H^+$-ATPase, even though subunit H is not a tyrosine-phosphorylated protein (Wong *et al.*, 2011). The region of PtpA required to bind H subunit was mapped at it C-terminal α-helix and is also independent of the presence of the PtpA catalytic cysteine (Wong *et al.*, 2011). Unfortunately, attempts to isolate a putative macrophage host cell substrate for Dpm by pull-down assays, similar to those performed with *M. tuberculosis* were unsuccessful (data not shown), and further experiments are underway to elucidate its molecular mechanism. In summary, our results indicate that Dpm is a novel effector protein contributing to the ability of *B. cenocepacia* to subvert the phagocytic pathway in macrophages by a mechanism that is independent of its predicted phosphatase activity.

**Acknowledgements**

The authors thank to D. Aubert, R. Rosales-Reyes, C. Schmerk and O. El-Halfawy for technical advice. This research was supported by grants from Cystic Fibrosis Canada and the United

Kingdom Cystic Fibrosis Trust. A. A. was supported by a Post Doctoral fellowship from the Government of Canada and from the Consejo Nacional de Ciencia y Tecnología of Mexico.

## References

**Abdulrahman, B. A., Khweek, A. A., Akhter, A. & other authors (2013).** Depletion of the ubiquitin-binding adaptor molecule SQSTM1/p62 from macrophages harboring cftr ΔF508 mutation improves the delivery of *Burkholderia cenocepacia* to the autophagic machinery. *J Biol Chem* **288**, 2049-2058.

**Al-Khodor, S., Marshall-Batty, K., Nair, V., Ding, L., Greenberg, D. E. & Fraser, I. D. (2013).** *Burkholderia cenocepacia* J2315 escapes to the cytosol and actively subverts autophagy in human macrophages. *Cell Microbiol* **16**, 378-395.

**Bach, H., Papavinasasundaram, K. G., Wong, D., Hmama, Z. & Av-Gay, Y. (2008).** *Mycobacterium tuberculosis* virulence is mediated by PtpA dephosphorylation of human vacuolar protein sorting 33B. *Cell Host Microbe* **3**, 316-322.

**Black, D. S. & Bliska, J. B. (1997).** Identification of p130Cas as a substrate of *Yersinia* YopH (Yop51), a bacterial protein tyrosine phosphatase that translocates into mammalian cells and targets focal adhesions. *EMBO J* **16**, 2730-2744.

**Bliska, J. B., Clemens, J. C., Dixon, J. E. & Falkow, S. (1992).** The *Yersinia* tyrosine phosphatase: specificity of a bacterial virulence determinant for phosphoproteins in the J774A.1 macrophage. *J Exp Med* **176**, 1625-1630.

**Böhmer, F., Szedlacsek, S., Tabernero, L., Ostman, A. & den Hertog, J. (2013).** Protein tyrosine phosphatase structure-function relationships in regulation and pathogenesis. *FEBS J* **280**, 413-431.

**Coenye, T. & Vandamme, P. (2003).** Diversity and significance of *Burkholderia* species occupying diverse ecological niches. *Environ Microbiol* **5**, 719-729.

**Courtney, J. M., Dunbar, K. E., McDowell, A., Moore, J. E., Warke, T. J., Stevenson, M. & Elborn, J. S. (2004).** Clinical outcome of *Burkholderia cepacia* complex infection in cystic fibrosis adults. *J Cyst Fibros* **3**, 93-98.

**Cowley, S. C., Babakaiff, R. & Av-Gay, Y. (2002).** Expression and localization of the *Mycobacterium tuberculosis* protein tyrosine phosphatase PtpA. *Res Microbiol* **153**, 233-241.

**Cozzone, A. J., Grangeasse, C., Doublet, P. & Duclos, B. (2004).** Protein phosphorylation on tyrosine in bacteria. *Arch Microbiol* **181**, 171-181.

**Cozzone, A. J. (2005).** Role of protein phosphorylation on serine/threonine and tyrosine in the virulence of bacterial pathogens. *J Mol Microbiol Biotechnol* **9**, 198-213.

**Craig, F. F., Coote, J. G., Parton, R., Freer, J. H. & Gilmour, N. J. (1989).** A plasmid which can be transferred between *Escherichia coli* and *Pasteurella haemolytica* by electroporation and conjugation. *J Gen Microbiol* **135**, 2885-2890.

**Drevinek, P. & Mahenthiralingam, E. (2010).** *Burkholderia cenocepacia* in cystic fibrosis: epidemiology and molecular mechanisms of virulence. *Clin Microbiol Infect* **16**, 821-830.

**Dziewit, L., Jazurek, M., Drewniak, L., Baj, J. & Bartosik, D. (2007).** The SXT conjugative element and linear prophage N15 encode toxin-antitoxin-stabilizing systems homologous to the tad-ata module of the *Paracoccus aminophilus* plasmid pAMI2. *J Bacteriol* **189**, 1983-1997.

**Ferreira, A. S., Leitão, J. H., Sousa, S. A., Cosme, A. M., Sá-Correia, I. & Moreira, L. M. (2007).** Functional analysis of *Burkholderia cepacia* genes *bceD* and *bceF*, encoding a phosphotyrosine phosphatase and a tyrosine autokinase, respectively: role in exopolysaccharide biosynthesis and biofilm formation. *Appl Environ Microbiol* **73**, 524-534.

**Ferreira, A. S., Leitão, J. H., Silva, I. N., Pinheiro, P. F., Sousa, S. A., Ramos, C. G. & Moreira, L. M. (2010).** Distribution of cepacian biosynthesis genes among environmental and clinical *Burkholderia* strains and role of cepacian exopolysaccharide in resistance to stress conditions. *Appl Environ Microbiol* **76**, 441-450.

**Figurski, D. H. & Helinski, D. R. (1979).** Replication of an origin-containing derivative of plasmid RK2 dependent on a plasmid function provided in trans. *Proc Natl Acad Sci U S A* **76**, 1648-1652.

**Flannagan, R. S., Linn, T. & Valvano, M. A. (2008).** A system for the construction of targeted unmarked gene deletions in the genus *Burkholderia*. *Environ Microbiol* **10**, 1652-1660.

**Flannagan, R. S., Jaumouillé, V., Huynh, K. K., Plumb, J. D., Downey, G. P., Valvano, M. A. & Grinstein, S. (2012).** *Burkholderia cenocepacia* disrupts host cell actin cytoskeleton by inactivating Rac and Cdc42. *Cell Microbiol* **14**, 239-254.

**George, A. M., Jones, P. M. & Middleton, P. G. (2009).** Cystic fibrosis infections: treatment strategies and prospects. *FEMS Microbiol Lett* **300**, 153-164.

**Govan, J. R., Brown, A. R. & Jones, A. M. (2007).** Evolving epidemiology of *Pseudomonas aeruginosa* and the *Burkholderia cepacia* complex in cystic fibrosis lung infection. *Future Microbiol* **2**, 153-164.

**Hamad, M. A., Skeldon, A. M. & Valvano, M. A. (2010).** Construction of aminoglycoside-sensitive *Burkholderia cenocepacia* strains for use in studies of intracellular bacteria with the gentamicin protection assay. *Appl Environ Microbiol* **76**, 3170-3176.

**Hume, D. A., Ross, I. L., Himes, S. R., Sasmono, R. T., Wells, C. A. & Ravasi, T. (2002).** The mononuclear phagocyte system revisited. *J Leukoc Biol* **72**, 621-627.

**Humphreys, D., Hume, P. J. & Koronakis, V. (2009).** The *Salmonella* effector SptP dephosphorylates host AAA+ ATPase VCP to promote development of its intracellular replicative niche. *Cell Host Microbe* **5**, 225-233.

**Huynh, K. K., Plumb, J. D., Downey, G. P., Valvano, M. A. & Grinstein, S. (2010).** Inactivation of macrophage Rab7 by *Burkholderia cenocepacia*. *J Innate Immun* **2**, 522-533.

**Jensch, F. & Kemper, B. (1986).** Endonuclease VII resolves Y-junctions in branched DNA in vitro. *EMBO J* **5**, 181-189.

**Keith, K. E., Hynes, D. W., Sholdice, J. E. & Valvano, M. A. (2009).** Delayed association of the NADPH oxidase complex with macrophage vacuoles containing the opportunistic pathogen *Burkholderia cenocepacia*. *Microbiology* **155**, 1004-1015.

**Kinchen, J. M. & Ravichandran, K. S. (2008).** Phagosome maturation: going through the acid test. *Nat Rev Mol Cell Biol* **9**, 781-795.

**Lamothe, J., Huynh, K. K., Grinstein, S. & Valvano, M. A. (2007).** Intracellular survival of *Burkholderia cenocepacia* in macrophages is associated with a delay in the maturation of bacteria-containing vacuoles. *Cell Microbiol* **9**, 40-53.

**Lamothe, J. & Valvano, M. A. (2008).** *Burkholderia cenocepacia*-induced delay of acidification and phagolysosomal fusion in cystic fibrosis transmembrane conductance regulator (CFTR)-defective macrophages. *Microbiology* **154**, 3825-3834.

**Lin, S. L., Le, T. X. & Cowen, D. S. (2003).** SptP, a *Salmonella typhimurium* type III-secreted protein, inhibits the mitogen-activated protein kinase pathway by inhibiting Raf activation. *Cell Microbiol* **5**, 267-275.

**Lipuma, J. J. (2005).** Update on the *Burkholderia cepacia* complex. *Curr Opin Pulm Med* **11**, 528-533.

**Loutet, S. A. & Valvano, M. A. (2010).** A decade of *Burkholderia cenocepacia* virulence determinant research. *Infect Immun* **78**, 4088-4100.

**Mahenthiralingam, E., Coenye, T., Chung, J. W., Speert, D. P., Govan, J. R., Taylor, P. & Vandamme, P. (2000).** Diagnostically and experimentally useful panel of strains from the *Burkholderia cepacia* complex. *J Clin Microbiol* **38**, 910-913.

**Mahenthiralingam, E., Vandamme, P., Campbell, M. E. & other authors (2001).** Infection with *Burkholderia cepacia* complex genomovars in patients with cystic fibrosis: virulent transmissible strains of genomovar III can replace *Burkholderia multivorans*. *Clin Infect Dis* **33**, 1469-1475.

**Mahenthiralingam, E., Baldwin, A. & Dowson, C. G. (2008).** *Burkholderia cepacia* complex bacteria: opportunistic pathogens with important natural biology. *J Appl Microbiol* **104**, 1539-1551.

**Marchler-Bauer, A., Lu, S., Anderson, J. B. & other authors (2011).** CDD: a Conserved Domain Database for the functional annotation of proteins. *Nucleic Acids Res* **39**, D225-229.

**Marolda, C. L., Hauröder, B., John, M. A., Michel, R. & Valvano, M. A. (1999).** Intracellular survival and saprophytic growth of isolates from the *Burkholderia cepacia* complex in free-living amoebae. *Microbiology* **145**, 1509-1517.

**Moreira, L. M., Videira, P. A., Sousa, S. A., Leitão, J. H., Cunha, M. V. & Sá-Correia, I. (2003).** Identification and physical organization of the gene cluster involved in the biosynthesis of *Burkholderia cepacia* complex exopolysaccharide. *Biochem Biophys Res Commun* **312**, 323-333.

**Morona, J. K., Morona, R., Miller, D. C. & Paton, J. C. (2002).** *Streptococcus pneumoniae* capsule biosynthesis protein CpsB is a novel manganese-dependent phosphotyrosine-protein phosphatase. *J Bacteriol* **184**, 577-583.

**Mukhopadhyay, A. & Kennelly, P. J. (2011).** A low molecular weight protein tyrosine phosphatase from *Synechocystis sp*. strain PCC 6803: enzymatic characterization and identification of its potential substrates. *J Biochem* **149**, 551-562.

**Murli, S., Watson, R. O. & Galán, J. E. (2001).** Role of tyrosine kinases and the tyrosine phosphatase SptP in the interaction of *Salmonella* with host cells. *Cell Microbiol* **3**, 795-810.

**Parke, J. L. & Gurian-Sherman, D. (2001).** Diversity of the *Burkholderia cepacia* complex and implications for risk assessment of biological control strains. *Annu Rev Phytopathol* **39**, 225-258.

**Persson, C., Carballeira, N., Wolf-Watz, H. & Fällman, M. (1997).** The PTPase YopH inhibits uptake of *Yersinia*, tyrosine phosphorylation of p130Cas and FAK, and the associated accumulation of these proteins in peripheral focal adhesions. *EMBO J* **16**, 2307-2318.

**Raugei, G., Ramponi, G. & Chiarugi, P. (2002).** Low molecular weight protein tyrosine phosphatases: small, but smart. *Cell Mol Life Sci* **59**, 941-949.

**Rosales-Reyes, R., Aubert, D. F., Tolman, J. S., Amer, A. O. & Valvano, M. A. (2012a).** *Burkholderia cenocepacia* type VI secretion system mediates escape of type II secreted proteins into the cytoplasm of infected macrophages. *PLoS One* **7**, e41726.

**Rosales-Reyes, R., Skeldon, A. M., Aubert, D. F. & Valvano, M. A. (2012b).** The Type VI secretion system of *Burkholderia cenocepacia* affects multiple Rho family GTPases disrupting the actin cytoskeleton and the assembly of NADPH oxidase complex in macrophages. *Cell Microbiol* **14**, 255-273.

**Saldías, M. S. & Valvano, M. A. (2009).** Interactions of *Burkholderia cenocepacia* and other *Burkholderia cepacia* complex bacteria with epithelial and phagocytic cells. *Microbiology* **155**, 2809-2817.

**Sambrook, J. & Russell, D. W. (2001).** *Molecular cloning. A laboratory manual*, Third edn. New York, USA: Cold Spring Harbor Laboratory Press.

**Schmerk, C. L. & Valvano, M. A. (2013).** *Burkholderia multivorans* survival and trafficking within macrophages. *J Med Microbiol* **62**, 173-184.

**Shi, L., Potts, M. & Kennelly, P. J. (1998).** The serine, threonine, and/or tyrosine-specific protein kinases and protein phosphatases of prokaryotic organisms: a family portrait. *FEMS Microbiol Rev* **22**, 229-253.

**Ueda, A. & Wood, T. K. (2009).** Connecting quorum sensing, c-di-GMP, pel polysaccharide, and biofilm formation in *Pseudomonas aeruginosa* through tyrosine phosphatase TpbA (PA3885). *PLoS Pathog* **5**, e1000483.

**Valvano, M. A., Rosales-Reyes, R., Schmerk, C. L. & Ostapska, H. (2014).** Molecular mechanisms of *Burkholderia cepacia* complex intracellular survival in phagocytic cells. In *From Genomes to Function*. Edited by T. Coeyne & E. Mahenthiralingam. Norwich, UK: Horizon Scientific Press.

**Vandamme, P., Holmes, B., Vancanneyt, M. & other authors (1997).** Occurrence of multiple genomovars of *Burkholderia cepacia* in cystic fibrosis patients and proposal of *Burkholderia multivorans* sp. *nov*. *Int J Syst Bacteriol* **47**, 1188-1200.

**Vergunst, A. C., Meijer, A. H., Renshaw, S. A. & O'Callaghan, D. (2010).** *Burkholderia cenocepacia* creates an intramacrophage replication niche in zebrafish embryos, followed by bacterial dissemination and establishment of systemic infection. *Infect Immun* **78**, 1495-1508.

**Vincent, C., Doublet, P., Grangeasse, C., Vaganay, E., Cozzone, A. J. & Duclos, B. (1999).** Cells of *Escherichia coli* contain a protein-tyrosine kinase, Wzc, and a phosphotyrosine-protein phosphatase, Wzb. *J Bacteriol* **181**, 3472-3477.

**Wang, S., Tabernero, L., Zhang, M., Harms, E., Van Etten, R. L. & Stauffacher, C. V. (2000).** Crystal structures of a low-molecular weight protein tyrosine phosphatase from *Saccharomyces cerevisiae* and its complex with the substrate *p*-nitrophenyl phosphate. *Biochemistry* **39**, 1903-1914.

**Wang, T., Ming, Z., Xiaochun, W. & Hong, W. (2011).** Rab7: role of its protein interaction cascades in endo-lysosomal traffic. *Cell Signal* **23**, 516-521.

**Waters, V. & Ratjen, F. (2006).** Multidrug-resistant organisms in cystic fibrosis: management and infection-control issues. *Expert Rev Anti-infect Ther* **4**, 807-819.

**Whitmore, S. E. & Lamont, R. J. (2012).** Tyrosine phosphorylation and bacterial virulence. *Int J Oral Sci* **4**, 1-6.

**Wong, D., Bach, H., Sun, J., Hmama, Z. & Av-Gay, Y. (2011).** *Mycobacterium tuberculosis* protein tyrosine phosphatase (PtpA) excludes host vacuolar-H+-ATPase to inhibit phagosome acidification. *Proc Natl Acad Sci U S A* **108**, 19371-19376.

**Zhou, B., He, Y., Zhang, X. & other authors (2010).** Targeting mycobacterium protein tyrosine phosphatase B for antituberculosis agents. *Proc Natl Acad Sci U S A* **107**, 4573-4578.

**Table 1. Strains and plasmids**

| Strain or plasmid | Relevant characteristics[a] | Source/reference |
|---|---|---|
| *B. cenocepacia* | | |
| K56-2 | ET12 clone related to J2315, clinical isolate | BCRRC[a],(Mahenthiraling am *et al.*, 2000) |
| MH1K | K56-2, Δ*amrABC*; $Gm^S$ | (Hamad *et al.*, 2010) |
| Δ*BCAL2200* | MH1K, Δ*BCAL2200*, $Gm^S$ | This study |
| Δ*BCAM0208* | MH1K, Δ*BCAM0208*, $Gm^S$ | This study |
| Δ*bceD* | MH1K, Δ*bceD*, $Gm^S$ | This study |
| Δ*dpm* | MH1K, Δ*dpm*, $Gm^S$ | This study |
| *B. multivorans* | | |
| ATCC 17616 $Gm^s$ | ATCC 17616, Δ*Bmul*_1614-1616, $Gm^S$ | (Schmerk & Valvano, 2013) |
| *E. coli* | | |
| BL21(DE3) | $F^-$ *dcm ompT hsd*S($r_B^-$,$m_B^-$) *gal* λ(DE3) | Stratagene |
| DH5α | $F^-$ ϕ80d*lacZ*Δ*M15* Δ(*lacZYA-argF*)*U169 endA1 recA1 hsdR*17($r_K^-$ $m_K^+$) *supE44 thi-1* Δ*gyrA96 relA1* | Laboratory stock |
| GT115 | $F^-$ *mcrA* Δ(*mrr-hsdRMS-mcrBC*) ϕ80d*lacZ*Δ*M15* Δ*lacX74 recA1 rspL* (*StrA*) *endA1* Δ*dcm idA*(Δ*MluI*)::*pir*-116 Δ*sbcC-sbcD* | Invitrogen |
| Plasmids | | |
| pDAI-SceI-SacB | $ori_{pBBR}$, $Tet^R$, *Pdhfr*, *mob*+, expressing I-SceI, SacB | (Hamad *et al.*, 2010) |
| pDA17 | Expression vector, $ori_{pBBR1}$, $Tet^R$, $mob^+$, $P_{dhfr}$, FLAG epitope | D. Aubert, unpublished |
| pET28 | Expression vector, $ori_{pBBR1}$, $Kan^R$, $P_{T7}$ | Novagen |
| pGPI-SceI | $ori_{R6K}$, $\Omega Tp^R$, *mob*+, I-SceI restriction site, $Tp^R$ | (Flannagan *et al.*, 2008) |
| pIN62 | $ori_{pBBR}$ $mob^+$, $Cm^R$, *DSRed* | (Vergunst *et al.*, 2010) |
| pRK2013 | $ori_{colE1}$, RK2 derivative, $Kan^R$, *mob*+, *tra*+ | (Figurski & Helinski, 1979) |
| pDelM0208 | pGPI-SceI with fragments flanking the BCAM0208 | This study |
| pDelM0628 | pGPI-SceI with fragments flanking the *dpm* | This study |
| pDelM0857 | pGPI-SceI with fragments flanking the BCAM0857 | This study |
| pDelL2200 | pGPI-SceI with fragments flanking the BCAL2200 | This study |
| pbceD | pDA17 encoding *bceD* | This study |
| Pdpm | pDA17 encoding *dpm* | This study |
| pL2200 | pDA17 encoding *BCAL2200* | This study |
| pM0208 | pDA17 encoding *BCAM0208* | This study |
| pΔ27 | pDA17 encoding *dpm* without their first 27 codons | This study |
| pHisL2200 | pET28 encoding 6xHis-BCAL2200-FLAG tagged | This study |
| pHisdpm | pET28 encoding 6xHis-*dpm*-FLAG tagged | This study |
| pHisdpm D36C | pHisdpm, with the substitution D36C | This study |
| pdpmHis | pET28 encoding *dpm*-6xHis tagged | This study |
| pdpmHis D36C | pdpmHis, with the substitution D36C | This study |

[a]BCRRC, B. cepacia complex Research and Referral Repository for Canadian Cystic Fibrosis Clinics; Cm, chloramphenicol; Gm, gentamicin; Kan, kanamycin; Tet, tetracycline; Tp, trimethoprim.

745 **Table 2. Oligonucleotides primers**

| Primer no. | 5'–3' primer sequence[a] | Restriction enzyme[b] | Purpose |
|---|---|---|---|
| 5914 | TTTTGAATTCCGAGACAGCAACGGCGTGTA | *EcoR*I | Pair to amplify BCAM0208 |
| 5915 | TTTTCTCGAGGCACACGTTGCCTTCGCAGA | *Xho*I | upstream region |
| 5997 | TTTTCTCGAGGGCGCTGATCGATCTCGC | *Xho*I | Pair to amplify BCAM0208 |
| 5998 | TTTTTCTAGAGACGAACGCGCCGATCACC | *Xba*I | downstream region |
| 5855 | TTTTGAATTCGACCAGGAAGTGCTGCTGT | *EcoR*I | Pair to amplify *dpm* upstream |
| 5856 | TTTTCTCGAGGACCTTCTTCGGTTCGTC | *Xho*I | region |
| 5857 | TTTTCTCGAGCCGATCGACTTCTACGAA | *Xho*I | Pair to amplify *dpm* |
| 5858 | TTTTTCTAGAGTTCAGCCATTCGGTGAAAG | *Xba*I | downstream region |
| 5999 | TTTTGAATTCGGTACGAGGTCAAGGAGGT | *EcoR*I | Pair to amplify BCAL2200 |
| 6000 | TTTTCTCGAGAGATGTTGCCGAGACAGACG | *Xho*I | upstream region |
| 6001 | TTTTCTCGAGGAAGTGGCCGATCCGTATT | *Xho*I | Pair to amplify BCAL2200 |
| 6002 | TTTTTCTAGACACGGATTCGACGATTTCA | *Xba*I | downstream region |
| 6003 | TTTTGAATTCGCTCGAACGCCTCACCTT | *EcoR*I | Pair to amplify *bceD* |
| 6014 | TTTTCATATGGTGCGACTTGAACAGCATT | *Nde*I | upstream region |
| 6004 | TTTTCATATGGAACGTCTGGTTCAAGGATG | *Nde*I | Pair to amplify *bceD* |
| 6005 | TTTTTCTAGAGACCGATTGCGTCGTGTT | *Xba*I | downstream region |
| 6006 | TTTCATATGAAAAGAAGGCACACC | *Nde*I | Forward to *dpm* |
| 6007 | TTTTCTAGACTGCTTCGCCGGCAC | *Xba*I | Reverse to *dpm* |
| 6008 | TTTCATATGACCCGCGTTGCGATC | *Nde*I | Forward to BCAL2200 |
| 6025 | ACCGCTGAATACCGTGTCTAGAGCG | *Xba*I | Reverse to BCAL2200 |
| 6010 | TTTCATATGCCGACCCCGCCCCCG | *Nde*I | Forward to BCAM0208 |
| 6011 | TTTTCTAGATGACTGGAATCCTGAG | *Xba*I | Reverse to BCAM0208 |
| 6012 | TTTCATATGTTCCGGAACATCCTG | *Nde*I | Forward to *bceD* |
| 6013 | TTTTCTAGAGCATAGTTTCTGTAG | *Xba*I | Reverse to *bceD* |
| 6486 | TTTCATATGGAACCGAAGAAGGTCGCG | *Nde*I | Forward from codon 28 of *dpm* |
| 6829 | TTTCCATGGAAAGAAGGCACACCCTC | *Nco*I | Forward to *dpm* |
| 6830 | TTTCTCGAGCTGCTTCGCCGGCACGG | *Xho*I | Reverse to *dpm* |
| 6496 | AGGTCGCGTTCGTCTGCACGGGCAACACCG | N/A | Forward to exchange *dpm* D36C |
| 6517 | CGGTGTTGCCCGTGCAGACGAACGCGACCT | N/A | Reverse to exchange *dpm* D36C |

746 [a]Restriction endonuclease sites incorporated in the oligonucleotide sequences are underlined.
747 [b]N/A indicates the absence of restriction site.
748

**Figure Legends**

**Fig. 1.** *B. cenocepacia* J2315 genome encodes 4 predicted LMW-PTPs. (a). Partial ClustalW sequence alignment of *Burkholderia cenocepacia* Dpm, BCAM0208, BceD, BCAL2200, *Mycobacterium tuberculosis* PtpA (Mtb PtpA), *Saccharomyces cerevisiae* LTP1 (YEAST_LTP1), *Homo sapiens* LMWPc (HUMAN_LMWPc), and *Sus scrofa* LMWPc (SWINE_LMWPc). Bar indicates the tyrosine phosphatase motif, $CX_5R(S/T)$, and the asterisk denotes the position of the catalytic cysteine. (b) Schematic representation of the genetic environment around the predicted *B. cenocepacia* LMW-PTPs (black) and their associated tyrosine kinases (grey) as annotated in strain J2315. Predicted iron-sulfur metabolism related genes are marked by an asterisk. Arrows denote the directionality of gene transcription.

**Fig. 2.** Secretion of LMW-PTPs into the growth medium. pDA17 derivatives encoding the various predicted LMW-PTPs were expressed in *B. cenocepacia* K56-2. Immunodetection of whole-cell-lysates and secreted proteins was performed using antibodies specific for the FLAG epitope (α-FLAG) and the beta lactamase of *E. coli* (α-TEM-1). Molecular masses of protein standards are indicated.

**Fig. 3.** Characterization of single-deletion mutant strains. (a) Growth curves in LB medium at 37 °C (straight lines) and 42 °C (dashed lines). (b) Bacterial motility assays in soft agar at 37 °C. Graph represents the mean ± SEM from three independent experiments. *** $p<0.001$ relative to MH1K (WT).

**Fig. 4.** Bacterial colocalization with dextran-rich vacuoles. Pulse-chase experiments were conducted with RAW264.7 macrophages. Lysosomes were pre-loaded with fluorescein-dextran and infected with strains expressing the DSRed fluorescent protein. Colocalization was assessed at 2 h post infection. (a) Immunofluorescence microscopy images of infected macrophages with MH1K (wild-type) and Δ*dpm* strains. (b) Quantification of BcCV colocalizing with dextran at 2 h post infection. Graph represents the mean ± SEM from three independent experiments. ** $p<0.01$ relative to MH1K (WT).

**Fig. 5.** Colocalization of BcCVs with LAMP-1. RAW264.7 macrophages were infected with MH1K and Δ*dpm* strains expressing the DSRed fluorescent protein or Δ*dpm* expressing pdpm. (a) Colocalization at 2 h post infection. Cells were fixed and immunolabelled using rat anti-LAMP-1 and a secondary antibody conjugated to Alexa Fluor 488. For complementation assays *B. cenocepacia* did not express the DSRed encoding plasmid, as it was incompatible with the complementing plasmids. Therefore bacteria were detected in these cases by antiserum against K56-2, plus a secondary anti-rabbit antibody conjugated to Alexa Fluor 594. (b) Quantification of BcCVs colocalizing with LAMP-1 at 2 and 4 h post infection. Graph represents mean ± SEM from three independent experiments. ** $p<0.01$ relative to MH1K (WT).

**Fig. 6.** Secretion of Dpm during macrophage infection. (a) RAW264.7 macrophages were infected with Δ*dpm* carrying the plasmid pdpm or pΔ27 and examined for immunolocalization of the Dpm protein together with *B. cenocepacia* at 1 h post infection. (b) Quantification of FLAG colocalizing with BcCV. Graph represents mean ± SEM from three independent experiments. *** $p<0.001$ relative to FLAG colocalization of Δ*dpm* containing pdpm. (c) Secretion assays in *B. cenocepacia* expressing pdpm or pΔ27. Immunodetection of whole-cell-lysates and secreted

proteins was performed using antibodies specific for the FLAG epitope (α-FLAG) and the *E. coli* β-lactamase (α-TEM-1). Molecular masses of protein standards are indicated.

**Fig. 7.** Intramacrophage survival of *B. cenocepacia* mutants with deletion of LMW-PTPs encoding genes. Infected macrophages were lysed at 1 or 24 h post infection, and intracellular bacteria were enumerated by serial dilution and colony counts on LB agar plates. The results represent the averages and standard errors of three independent experiments. No significant differences in replication or survival were found using an unpaired *t* test.

**Fig. 8.** Dpm modifies *B. multivorans* phagosome traffic. (a) Pulse-chase experiments in RAW264.7 macrophages. Lysosomes were pre-loaded with fluorescein-dextran and infected with *B. multivorans* carrying pdpm or the vector pDA17. (b) Quantification of BmCV colocalization with dextran at 2 h post infection. Graph represents mean ± SEM from three independent experiments. *** $p<0.001$ relative to dextran colocalization of *B. multivorans* containing pDA17. (c) Immunodetection of Dpm in whole-cell-lysates (P) and supernatants (S) of *B. cenocepacia* and *B. multivorans* carrying pdpm. Detection was performed using antibodies specific for the FLAG epitope (α-FLAG) and the α subunit of the *E. coli* RNA polymerase (α-RNAPol) as cell lysis control. Molecular masses of protein standards are indicated at the left of each panel.

**Fig. 9.** Phosphatase activity assay. (a) Coomassie blue-stained SDS-PAGE of purified Dpm and BCAL2200 recombinant proteins. (b) Phosphatase activity of purified BCAL2200 and Dpm at 37 °C using 1mM PNPP as substrate.

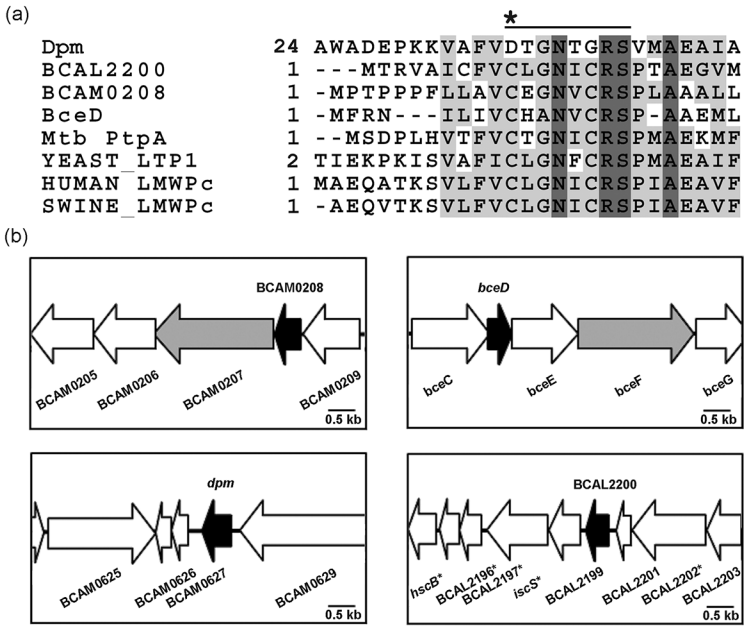
(a)
*
Dpm 24 AWADEPKKVAFVDTGNTGRSVMAEAIA
BCAL2200 1 ---MTRVAICFVCLGNICRSPTAEGVM
BCAM0208 1 -MPTPPPFLLAVCEGNVCRSPLAAALL
BceD 1 -MFRN---ILIVCHANVCRSP-AAEML
Mtb PtpA 1 --MSDPLHVTFVCTGNICRSPMAEKMF
YEAST_LTP1 2 TIEKPKISVAFICLGNFCRSPMAEAIF
HUMAN_LMWPc 1 MAEQATKSVLFVCLGNICRSPIAEAVF
SWINE_LMWPc 1 -AEQVTKSVLFVCLGNICRSPIAEAVF
(b)
BCAM0208
BCAM0205
BCAM0206
BCAM0207
BCAM0209
0.5 kb
bceD
bceC
bceE
bceF
bceG
0.5 kb
dpm
BCAM0625
BCAM0626
BCAM0627
BCAM0629
0.5 kb
BCAL2200
hscB*
BCAL2196*
BCAL2197*
iscS*
BCAL2199
BCAL2201
BCAL2202*
BCAL2203
0.5 kb

**Fig.1**

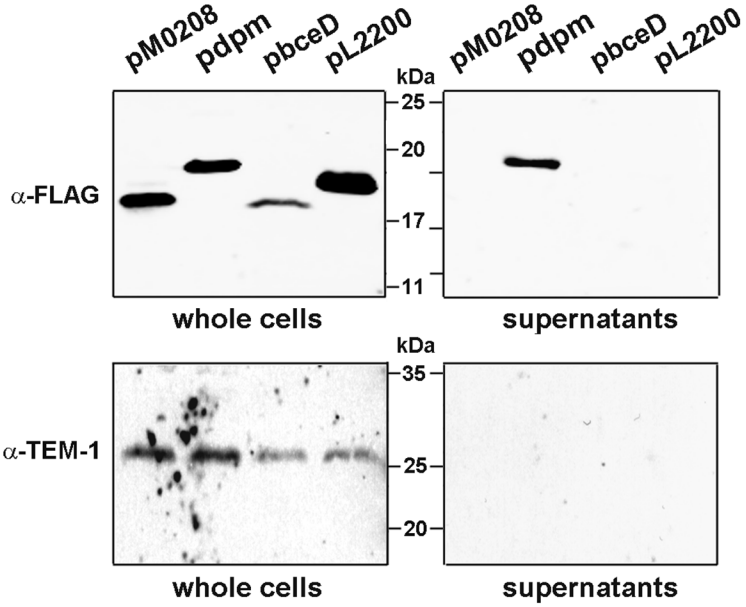
pM0208
pdpm
pbceD
pL2200
pM0208
pdpm
pbceD
pL2200
kDa
25
20
17
11
α-FLAG
whole cells
supernatants
kDa
35
25
20
α-TEM-1
whole cells
supernatants

**Fig. 2**

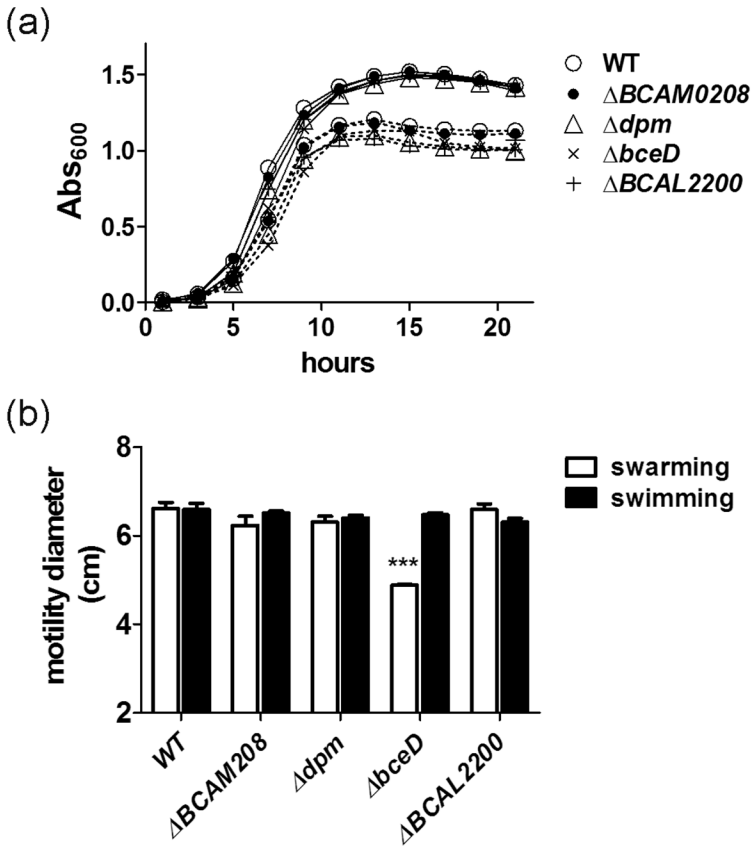
(a)
Abs600
1.5
1.0
0.5
0.0
0
5
10
15
20
hours
WT
ΔBCAM0208
Δdpm
ΔbceD
ΔBCAL2200
(b)
motility diameter (cm)
8
6
4
2
***
swarming
swimming
WT
ΔBCAM208
Δdpm
ΔbceD
ΔBCAL2200

823
824 **Fig. 3**

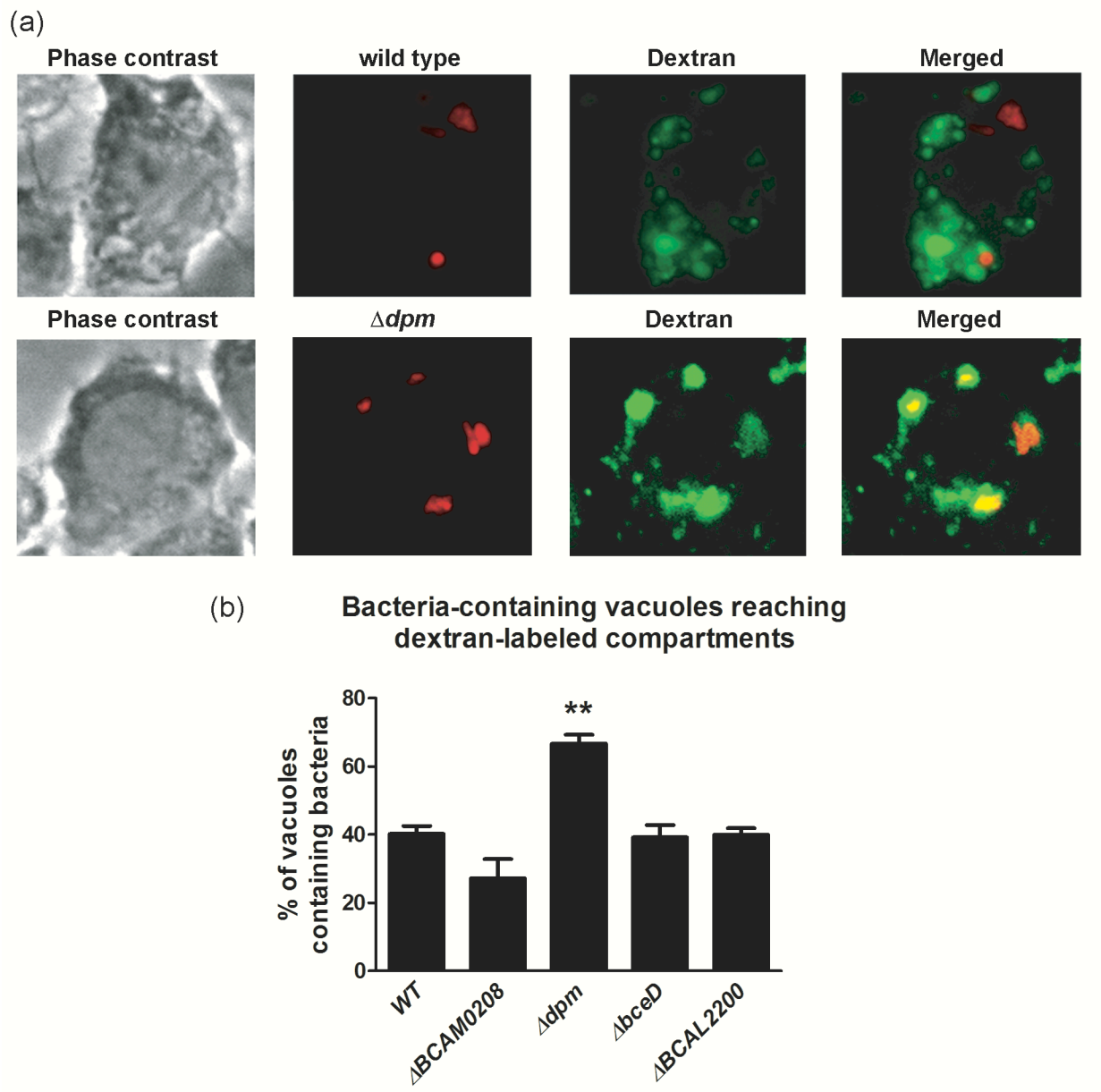
(a)
Phase contrast
wild type
Dextran
Merged
Phase contrast
Δdpm
Dextran
Merged
(b)
Bacteria-containing vacuoles reaching dextran-labeled compartments
% of vacuoles containing bacteria
80
60
40
20
0
**
WT
ΔBCAM0208
Δdpm
ΔbceD
ΔBCAL2200

825
826 **Fig. 4**

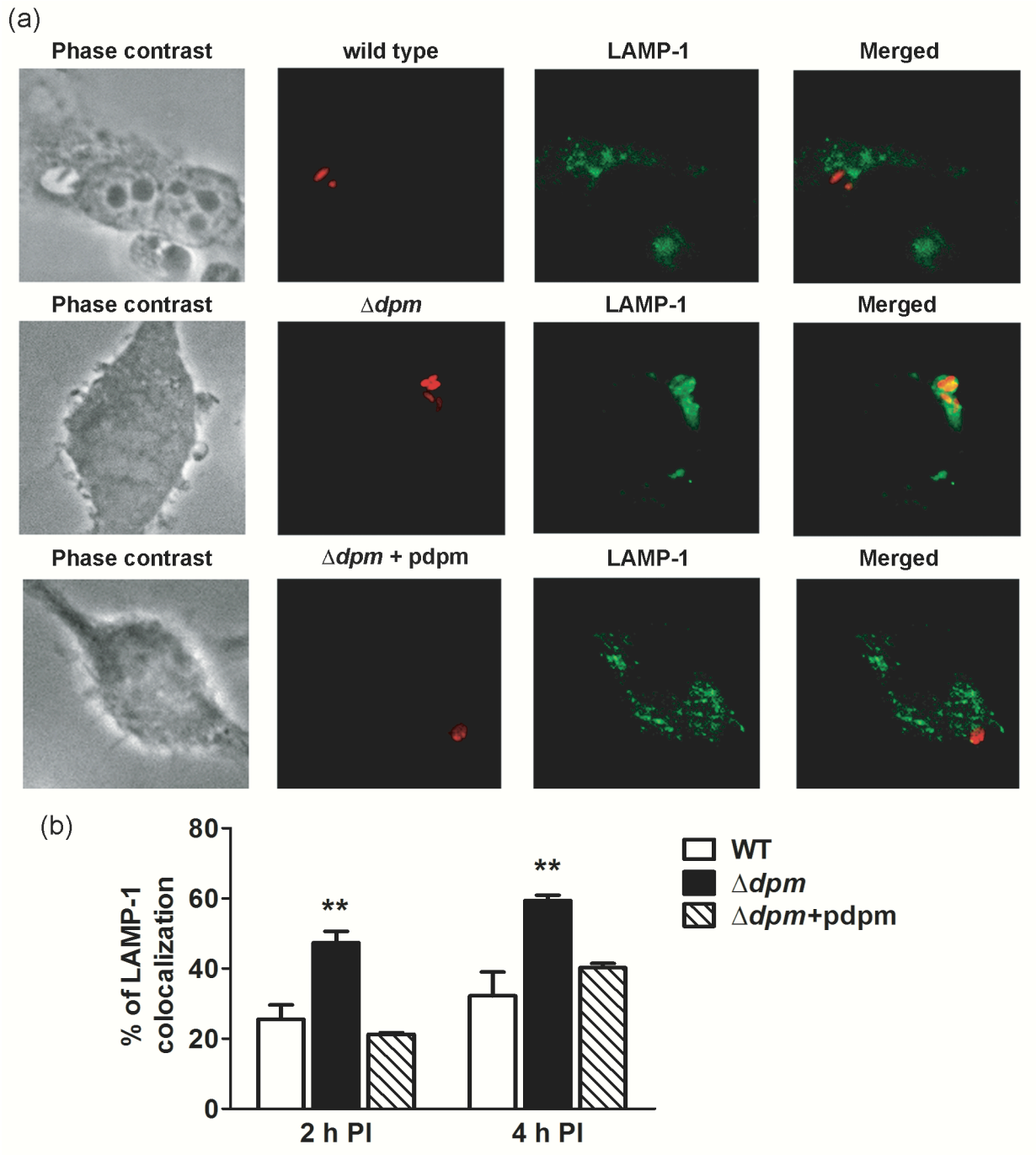
(a)
Phase contrast
wild type
LAMP-1
Merged
Phase contrast
Δdpm
LAMP-1
Merged
Phase contrast
Δdpm + pdpm
LAMP-1
Merged
(b)
% of LAMP-1 colocalization
80
60
40
20
0
**
**
2 h PI
4 h PI
WT
Δdpm
Δdpm+pdpm

827
828 **Fig. 5**

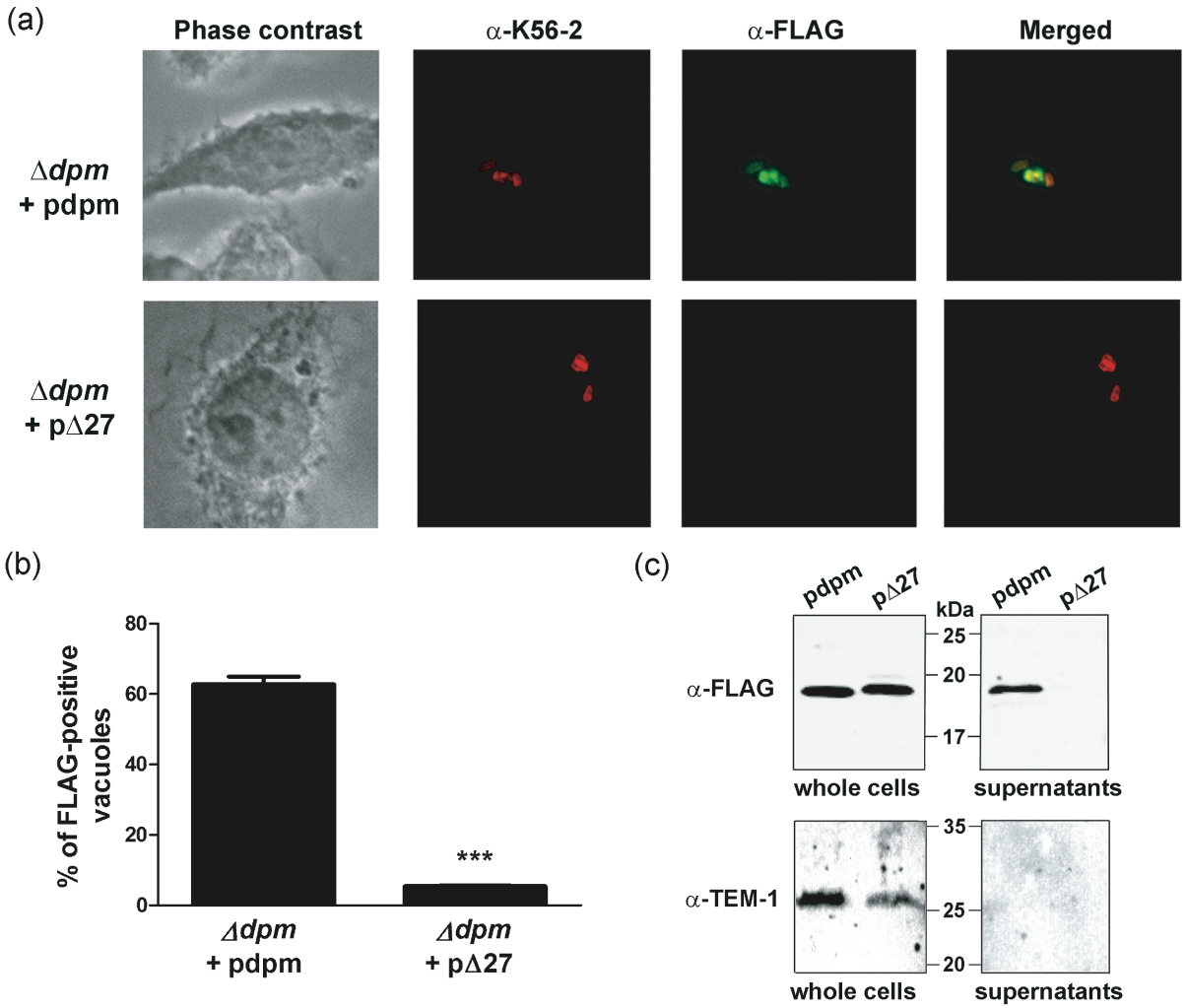


829
830 **Fig.6**
831

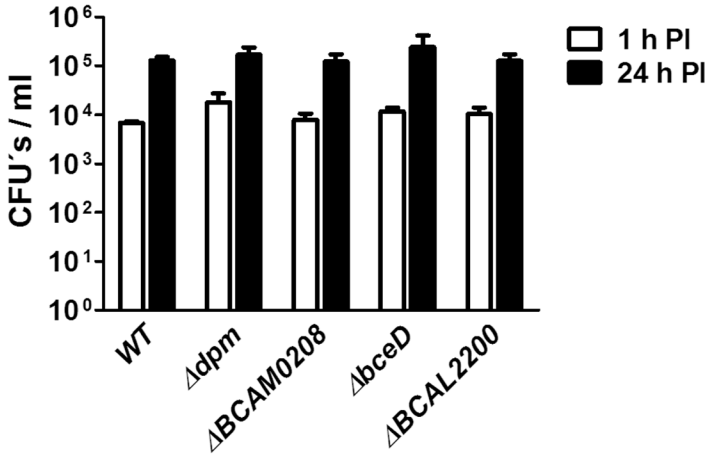


832
833 **Fig. 7**

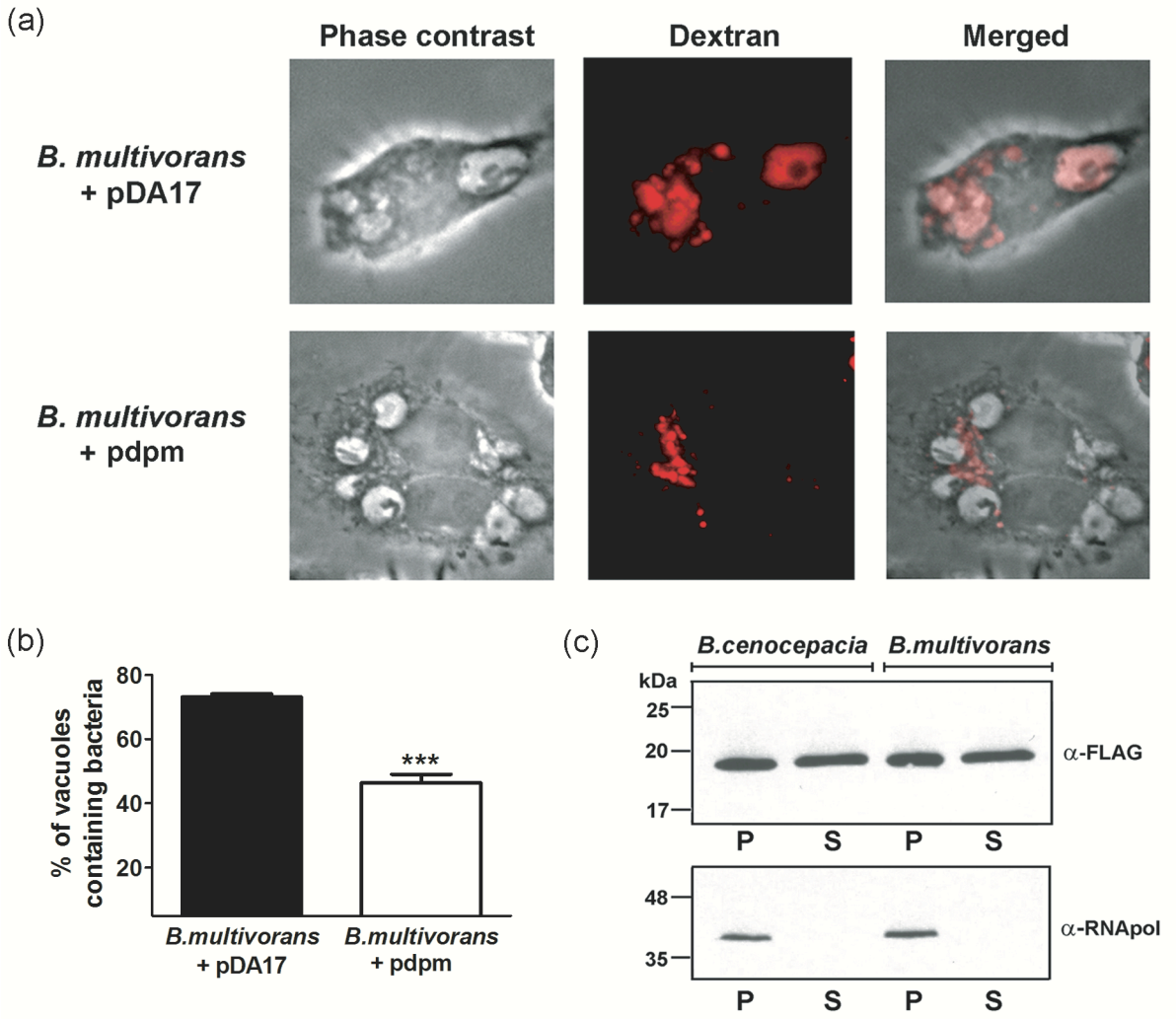


834
835 **Fig. 8**
836

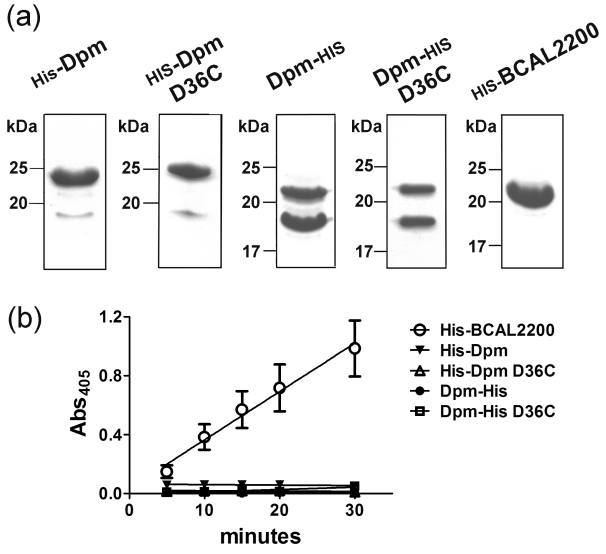


837
838 **Fig. 9**